Available online at www.sciencedirect.com
ScienceDirect
Journal of the European Ceramic Society 28 (2008) 1827–1838
www.elsevier.com/locate/jeurceramsoc

Poling of hard ferroelectric PZT ceramics

Talal M. Kamel, G. de With *

Laboratory of Materials and Interface Chemistry, Eindhoven University of Technology, 5600 MB Eindhoven, The Netherlands

Received 16 September 2007; received in revised form 14 November 2007; accepted 25 November 2007
Available online 4 March 2008

Abstract

Poling of hard ferroelectric ceramics is not an easy process. Pinning of domain walls due to defects prevents the material to be switched by moderate conditions of poling. In this paper, we try to explore a way to facilitate the poling process by defeating the counteracting defects in lead zirconate titanate (PZT). We focus on the structural and electrical effects that enhance the domain mobility, as reflected by hysteresis loops. Increased mobility leads to depinched hysteresis loops and consequently to easier poling and eventually to better piezoelectric properties. Different poling conditions were applied to ceramic samples sintered at different temperatures before and after hysteresis depinching. Dielectric parameters were measured after each poling state. The results showed that the hard ceramic can be efficiently polarized only after domain depinning, which can be done by various methods.

Keywords: Poling; PZT; Ferroelectrics; Domain walts; Depinning

1. Introduction

Domain walls in ferroelectrics are boundaries that separate domains polarized in different directions.[1] In soft ferroelectric ceramics, the domain walls move irreversibly in a semi-continuous way (yielding normal hysteresis loops). Hard materials are usually characterized by biased and/or pinched hysteresis loops because the domain walls are clamped and perform reversible movements around equilibrium configurations meanwhile discretely jumping from one configuration to another given sufficient energy. These equilibrium configurations are attributed to crystal lattice defects that act as pinning centres for the domain walls.

As is well known, a ferroelectric ceramic gets its useful piezoelectric properties by applying adequate poling conditions. Consequently, the piezoelectric properties are greatly dependent on the poling conditions.[2–8] It has been verified that there is a direct dependence between the dielectric and piezoelectric properties and the degree of domain orientation set by poling conditions.[9–15]

Poling of hard ferroelectric ceramics is not an easy process. Pinning of domain walls due to defects prevents the material to be switched by moderate poling conditions.[16] Unfortunately, literature on poling of hard ceramics is scarce. However, several authors[17–25] have discussed the defects in hard ceramics (e.g. lead zirconate titanate (PZT)) which are believed to be responsible for the difficult poling of these materials.

In the present work, we try to explore a way to facilitate the poling process by defeating the counteracting defects. Acceptor dopants for $Pb^{2+}(Zr^{4+}, Ti^{4+})O_3$ such as Fe^{3+} ions are compensated by oxygen vacancies. During sintering the (effectively negative) dopant ion ($Fe'_{Zr,Ti}$) and (effectively positive) oxygen vacancy ($V_O^{\bullet\bullet}$) form a defect-dipole ($Fe'_{Zr,Ti}$–$V_O^{\bullet\bullet}$). However, the oxygen vacancies are still movable below the Curie temperature (*i.e.* at room temperature) because an oxygen ion and an oxygen vacancy are only 2.8 Å apart and hopping easily occurs.[29] The orientation of defect-dipoles thus takes place via oxygen vacancy diffusion.[29] This diffusion leads to domain wall immobility and eventually a constricted hysteresis loops, low dielectric constant, low dielectric loss, low piezoelectric coupling factor and consequently acceptor doped PZT (or hard PZT as it is commonly named) are very difficult to polarize.[17] In the following, the models suggested for the role of defects in hard ferroelectric ceramics will be summarized.

* Corresponding author.
E-mail addresses: T.M.Kamel@tue.nl (T.M. Kamel), G.deWith@tue.nl (G. de With).

0955-2219/$ – see front matter © 2008 Elsevier Ltd. All rights reserved.
doi:10.1016/j.jeurceramsoc.2007.11.023

1.1. Models of domain wall stabilization

Lambeck and Jonker[20] showed that reorientation of defect-dipoles is expected to be responsible for domain stabilization. A perovskite lattice cell containing such defect-dipoles may remain paraelectric even if all neighbouring cells are ferroelectric.[16] In the paraelectric phase the oxygen vacancy may jump by thermal activation to the energetically equivalent neighbouring oxygen sites of the lattice cell, thus changing the orientation of the electric moment of the defect-dipole. Upon cooling from the paraelectric phase to the ferroelectric phase a spontaneous polarization P_S is established. The energy of the various orientations of the defect-dipoles then becomes different.

If the lattice has a polarization direction in the +*Z*-direction, three possible positions of the oxygen vacancy with three different energy levels are expected. If a transition takes place to a lower energy site, the oxygen vacancies may contribute to ageing of the ceramic.[16] Ageing is defined as the spontaneous change of a property with time under zero external stress and isothermal conditions.[21]

Many authors investigated the ageing behaviour and several plausible models have been developed to interpret this phenomenon. A quantitative theory about ageing is, however, not yet put forward. Most of the models are of a qualitative nature.

Carl and Härdtl[22] classified the mechanisms that may be responsible for the occurrence of domain wall stabilization in ferroelectric ceramics in three categories [22]:

(i) *Volume effect*. Ceramics always contain defects, intentional (*i.e.* doping) or unintentional (*i.e.* impurities), in the form of foreign atoms or vacancies. These defects can occupy energetically preferred sites in the lattice and favour a certain direction for the spontaneous polarization revealing itself experimentally as an internal bias.
(ii) *Domain effect*. This effect is also due to defects, which diffuse in the course of time into the domain walls and fix their position. The driving forces may be elastic (neutralization of internal stresses) or electric (compensation of electric charges, e.g. by valence changes of the foreign atoms).
(iii) *Grain boundary effect*. Several ferroelectric ceramics contain a secondary phase along the grain boundaries and/or on the triple points. Second phases lead to surface charges at the grain boundaries, which stabilize the domain configurations once these are established. During ageing the individual crystallite is biased by an overall preferred direction of polarization, but the individual domain walls remain mobile.

Robels and Arlt [23] showed that the ageing of the material with time corresponds to an increasing shift of the hysteresis loop along the *E*-axis. This shift is called the *internal bias field* E_i. The internal field in acceptor doped ceramics can be explained quantitatively[16] by oriented defect-dipoles. Domain clamping by orientation of defect-dipoles, according to Robels and Arlt,[23] occurs because a build up of E_i in time is realized by a slow relaxation of the defect-dipoles, which leads, in turn, to an increasing shift of the hysteresis loop along the *E*-axis. Therefore, the contribution of domain walls to the dielectric and piezoelectric properties should be decreasing with increasing orientation of the defects.[21,22]

In this paper, we focus on the structural and electrical effects that enhance the domain mobility, as reflected by hysteresis loops, that lead to depinched hysteresis loops and consequently to easier poling and eventually to better piezoelectric performance.

2. Experimental

2.1. Material

Modified PZT ($(Pb_{1-0.94}Sr_{0.06})\ (Fe_{0.008}\ Zr_xTi_{1-x-0.008})\ O_3$) ceramic powder, near the morphotropic phase boundary, coded *PXE43*, was provided by Morgan Electro Ceramics B.V. Eindhoven, The Netherlands. The powder was pressed into bars of at least 15 mm in diameter and sintered at different temperatures (1150–1300 °C) in a tube furnace with flowing oxygen. The bars were heated from room temperature to the desired temperature in 8 h, held at this temperature for 4 h and then cooled down to room temperature in 8 h. The sintered bars were diced into discs of 10 mm in diameter. Next, the discs were subjected to clean-firing at 700 °C for 48 h, cleaned in methanol in an ultrasonic bath for 2 min, washed in water and soap and dried in air. Finally, the discs were electroded with Ni by sputtering for electrical measurements.

The microstructure of the as-prepared samples was investigated using optical as well as scanning electron microscopy (JEOL, JSM 840A, Japan). The grain size d_{gs} was measured as a function of the sintering temperature using the mean linear intercept as grain size measure counting about 100 grains.

2.2. Hysteresis loop

Hysteresis loops were observed using a computer-controlled virtual ground method (*Radiant Technologies Inc.*, *RT6000 HVA-z 2000 V amplifier and RT6000 HVS-z high voltage input test system*) using the fast mode (0.4 ms) at different temperatures (RT–105 °C). The maximum applied electric field was 50 kV/cm. Silicone oil (*Wacker Silicone Fluid*, *AP 150*) was used as an insulating medium during the measurements. The loops were not completely closed due to the non-switchable polarization.[30,32]

2.3. Poling

As-prepared and aged samples were poled at different temperatures (70, 90, 100 °C). The poling electric field was kept constant over the whole poling process at 30 kV/cm. The sample is heated up to the desired temperature in the silicone oil bath under application of the electric field. The field increases at a constant rate of 10 V/s until it reaches 30 kV/cm. Then the sample is held under these conditions for 10 min. During the last minute the sample is cooled down, with the field still

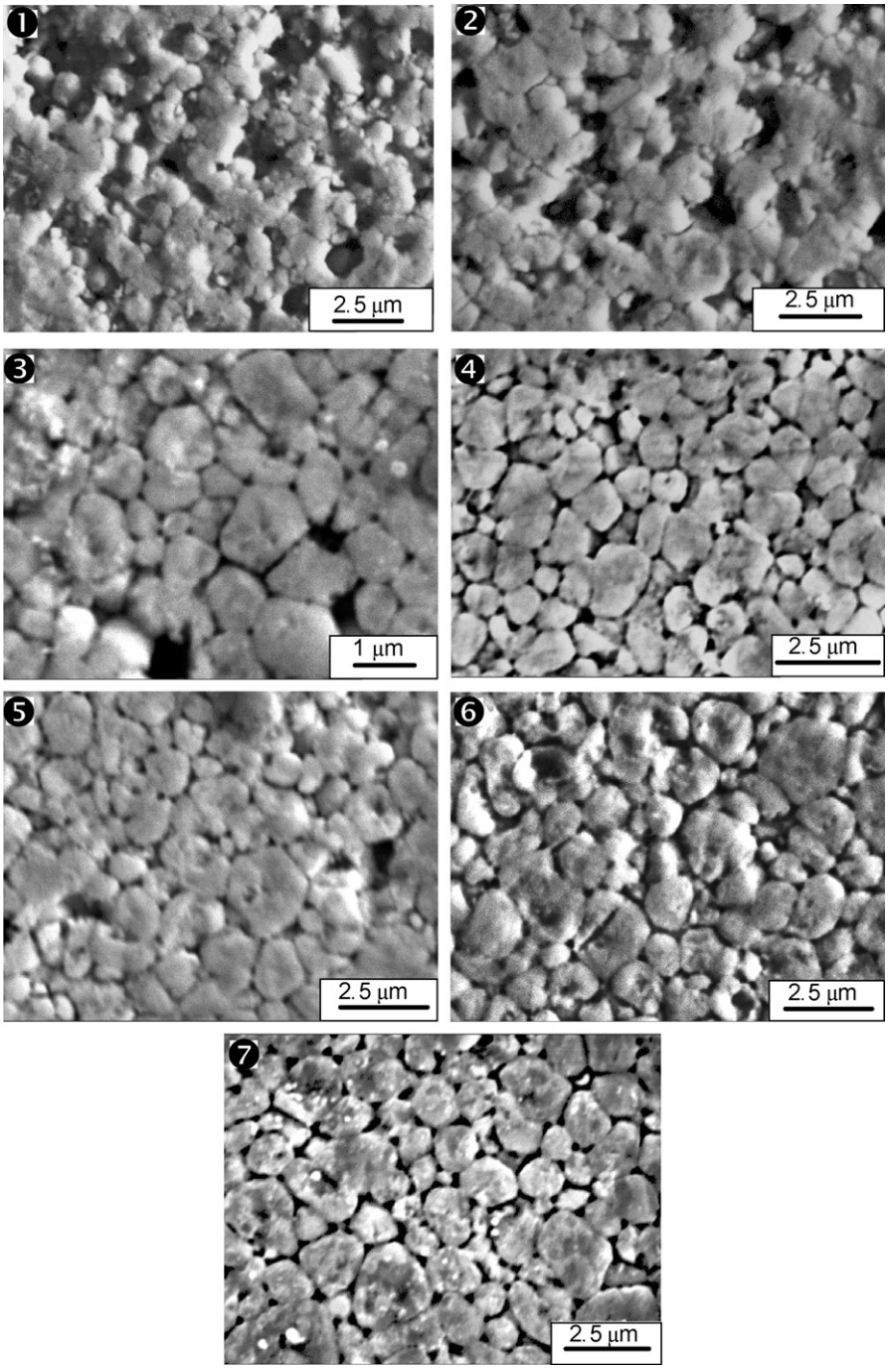

Fig. 1. SEM micrographs of Fe doped PZT samples sintered at: (1) 1150 °C, (2) 1175 °C, (3) 1200 °C, (4) 1225 °C, (5) 1250 °C, (6) 1275 °C, (7) 1300 °C.

applied, to room temperature where after the electric field is removed.

2.4. Dielectric, piezoelectric and pyroelectric properties

The dielectric and piezoelectric parameters (ε_r, $\tan\delta$, k_p, k_{33}, k_{eff}) of poled and (ε_r, $\tan\delta$) of non-poled samples were measured using a *HP4294A Precision Impedance Analyzer* at 1 kHz in the temperature range from room temperature up to 400 °C. The pyroelectric measurements were carried out using the direct method.[31] The setup used is described elsewhere.[3]

3. Results

3.1. Microstructure

Fig. 1(1–7) depicts the micrographs of the nonpoled samples. Table 1 shows the variation of the density and grain size with sintering temperature. The compacts showed a high densification at a sintering temperature above 1200 °C reaching a very dense structure at 1300 °C. However, there is not a significant variation in grain size because the grain growth is inhibited due to the acceptor doping.[17] The average grain size ranges from

Table 1
Sintering temperature and the corresponding resulting densities

Sample name	Sintering temperature (°C)	Grain size (μm)	Density (ρ_{exp}) (g/cm^3)	ρ_{exp}/ρ_{th} (%)
(1)	1150	[a]	6.48	82.65
(2)	1175	[a]	6.78	86.47
(3)	1200	0.91	7.13	90.94
(4)	1225	1.00	7.35	93.75
(5)	1250	1.34	7.59	96.81
(6)	1275	1.49	7.80	99.11
(7)	1300	1.70	7.82	99.74

[a] Due to the porous structure, the grain size could not be determined.

0.9 μm for 1200 °C to 1.7 μm for 1300 °C. The samples sintered at lower temperature showed a porous structure, so that the grain size could not even be determined properly.

3.2. Hysteresis loops after ageing

Fig. 2 shows the hysteresis loops of an aged sample at room temperature. A double hysteresis loop is the common characteristic of all samples. At room temperature the loops are constricted even at 50 kV/cm. Double (*pinched*) hysteresis loops are attributed to a reversible movement of domain walls as they are electrically and/or elastically[39] pinned by defects.

3.3. Poling effect after ageing

The dielectric constant ε_r, dielectric dissipation factor tan δ and the planar coupling factor k_p at room temperature as a function of the sintering temperature after poling at different temperatures are presented in Fig. 3(A–C). The dielectric and piezoelectric properties increase considerably due to enhanced domain wall mobility as a result of the decreasing of the number of pores. However, poling has a small influence. The dielectric dissipation factor tan δ shows anomalous behaviour as compared to the soft counterpart (PXE52)[3] as it increases by increasing the poling field which means that the domain walls are still movable or, rather more precisely, that full polarization is not yet reached. The noticeable low value of tan δ is attributed to ageing[21] and domain wall stabilization.[6,21,22] This observation is consistent with the constricted hysteresis loops shown in Fig. 2.

To determine the Curie transition temperature, the dielectric constant was measured as a function of temperature at 1 kHz, Fig. 4. As can be seen in this figure, the sample shows a typical ferroelectric phase transition peak at a Curie transition temperature of 335 °C. The onset of the paraelectric phase state is accompanied with the disappearance of the electromechanical coupling factor k_p. This rules out any other possible causes for the anomalous behaviour of the hysteresis loops at room temperature, e.g. *antiferroelectricity*.

3.4. Hysteresis loop depinching

It is widely known that there are only two ways for depinching the hysteresis loop.[1] Electrically, by repeated cycling (hundred or even thousands of times) of the hysteresis loop, the pinching will disappear and the internal bias will be reduced.[1,20–22,32,34,35] This process is normally done above the Curie temperature[20,21]

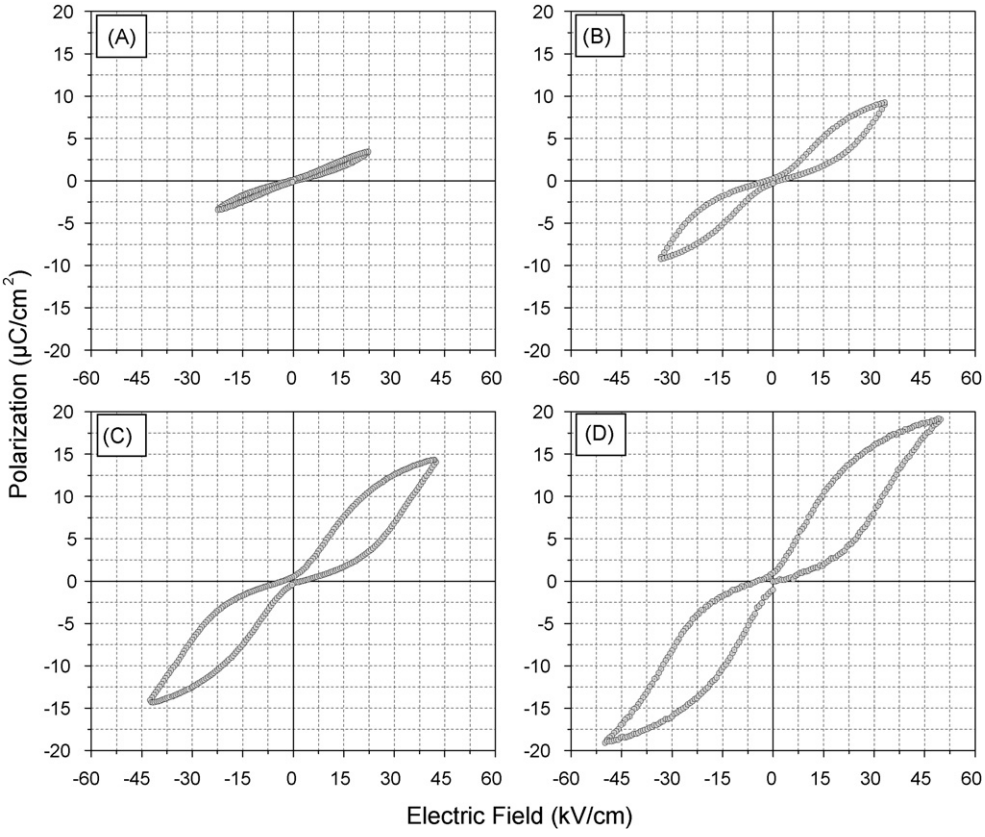

Fig. 2. Hysteresis loops for increasing maximum field of a non-poled sample (6) at room temperature. Sintering temperature: 1275 °C.

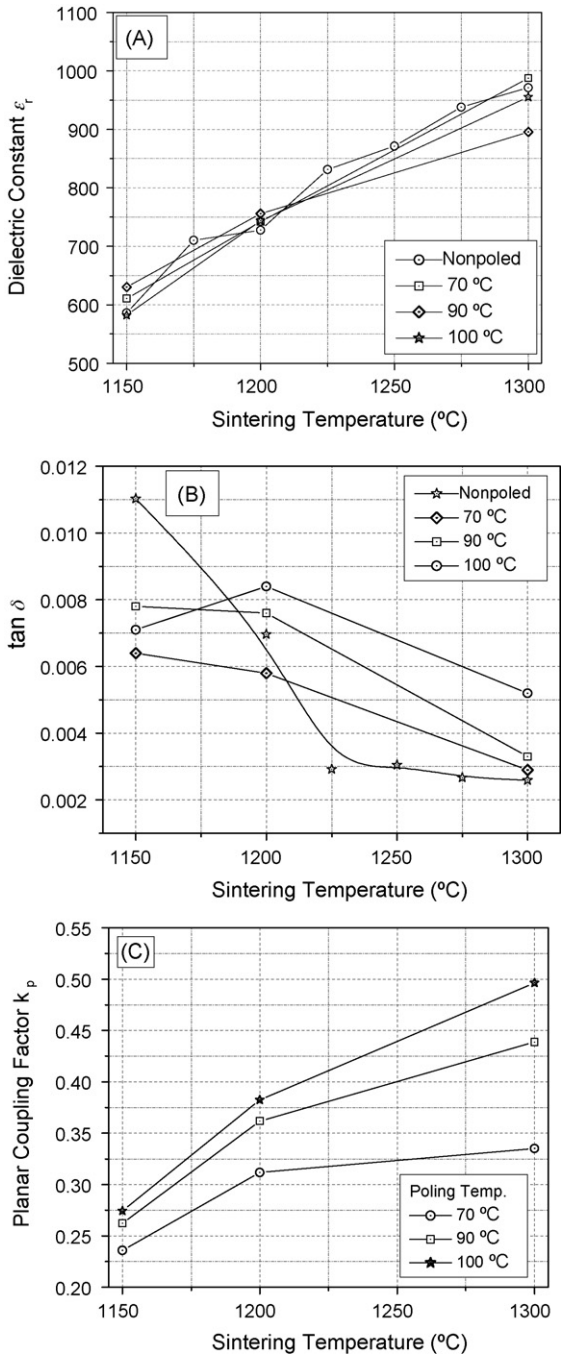

Fig. 3. Dielectric constant ε_r (A), dielectric loss tan δ (B) and planar electromechanical coupling factor k_p (C) after direct poling at different temperatures.

and is called *hysteresis relaxation*.[20,22] The relaxation of the internal bias E_i obeys, according to Carl and Härdtl[22]:

$$E_i(t) = E_i(0)\exp\left(-\frac{t}{\tau}\right) \quad (1)$$

The relaxation time τ depends on the temperature and the maximum applied electric field (*i.e.* relaxation is a thermally and electrically activated process). In some cases the depinching cannot be completely relaxed even after a large number of cycles.[1] The pinning can also be structurally removed by quenching the sample from well above the Curie temperature to

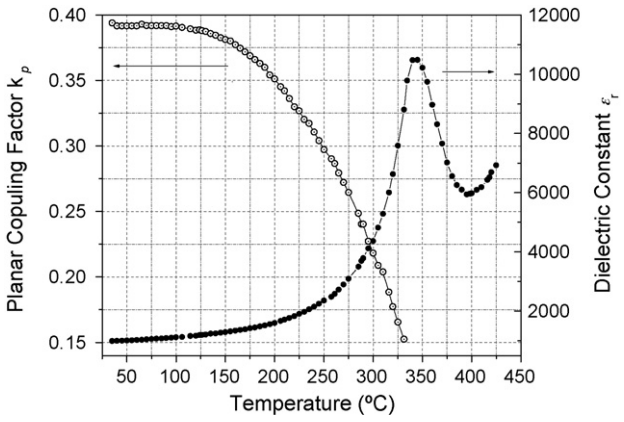

Fig. 4. Dielectric constant ε_r and the planar electromechanical coupling factor k_p as a function of temperature for sample poled at 30 kV/cm and 70 °C after electric depinning (50 kV/cm, 105 °C).

room temperature.[1,19] This effect is called *thermal relaxation*.[20,21]

However, we have found, in our case, that the loop can be gradually depinched by increasing the temperature up to the poling temperature, which is only one-third of the Curie temperature, and with no need of repeated cycling. The loop is gradually changed to normal shape by increasing the temperature, Fig. 5, and the applied field, Fig. 6. It can be easily noticed that, there is a transition temperature of about 95 °C at which (along with the highest applied field) the pinched loop can be relaxed by thermal activation. In other words, assuming a maximum applied electric field, the remanent polarization increases from zero to non-zero by increasing temperature and/or by the density, Fig. 7. The bias internal electric field before poling, as calculated according to Refs. [16,22], is significantly decreasing with increasing density of the ceramic, Fig. 9. At low ceramic density, the pores are abundantly present and therefore the domain wall mobility may be hindered because of space charges that accumulate on the pores.[17,33,39] Nevertheless, for more dense samples, hysteresis relaxation was found to be effective for depinching and lowering the internal bias. It was found that, the internal bias can be greatly reduced after quenching from 500 °C, well above the T_C of ~330 °C, to room temperature. The hysteresis loops after quenching are shown in Fig. 8. Fig. 9 shows the internal bias after quenching as a function of the sintering temperature. The internal bias slightly decreases in a nearly linear manner with increasing density. Due to the fast cooling ordering of the oxygen vacancies or their dipoles are hindered.[19] Consequently, the ceramic after the quenching process is in a metastable state.

3.5. Poling effect after de-ageing

3.5.1. Hysteresis loops

Hard ceramics can be poled into a stable state after de-ageing. After hysteresis depinching by our method the ceramic can be subjected to the normal poling procedure described above. Fig. 10 shows the *P–E* curves at room temperature after poling at 100 °C under an applied field of 30 kV/cm and field cooled. It is seen that a strong asymmetric polarization hysteresis curve

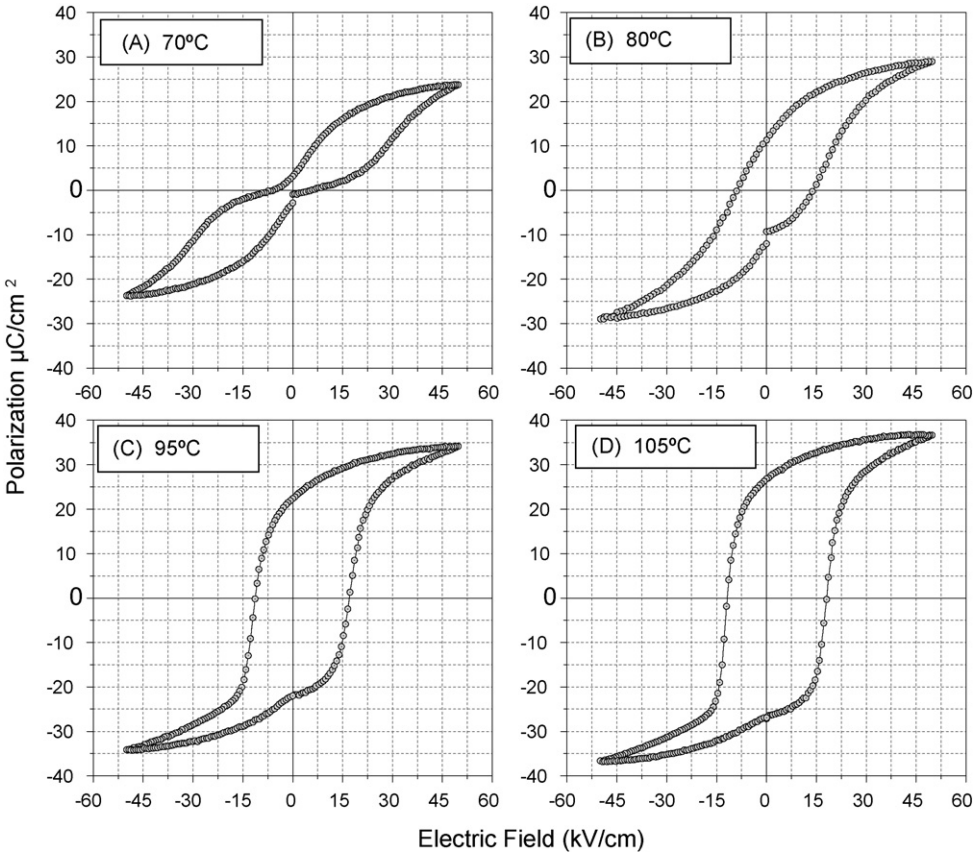

Fig. 5. Hysteresis loops at different temperatures of a non-poled sample (7) at the maximum applied electric field of 50 kV/cm.

results, revealing a unipolar polarization orientation. Clearly, field cooling results in irreversible changes in the defect distributions and domain stability unless the temperature is increased to enhance defect mobility. A similar behaviour is observed by other workers.[35,36] The large field shift is due to domain pinning by defects. The defects rearrange with the ferroelectric polarization at higher temperature, and freeze-in upon cooling resulting a stabilized polarization.[36]

3.5.2. Dielectric and piezoelectric properties

The dielectric constant ε_r, dielectric dissipation factor $\tan\delta$ and the planar coupling factor k_p at room temperature as a function of the sintering temperature for specimens poled after electrical de-ageing at different temperatures are presented in Fig. 11A–C. There is no significant influence of the poling temperature as well as the de-ageing itself on the dielectric properties. Poling after de-ageing showed a small enhancement of the electromechanical coupling factor. Densification of the ceramics is still the main ruler of the improved piezoelectric properties. However, thermal relaxation (quenching) was found to be very effective for enhancing ε_r, $\tan\delta$ and k_p, Fig. 12A–C and Table 2.

By poling the samples after de-ageing, the electromechanical coupling factor increases significantly as compared to the aged state. Generally, we note that the thermally quenched hard ceramic samples behave qualitatively the same as soft materials. This behaviour can be attributed to the effect of oxygen vacancies acting as pinning centres disordered by thermal quenching and resulting in randomization of the energy profile for domain wall motion.[19]

3.5.3. Thermally stimulated discharge current (TSDC)

After electrical depinning, thermally stimulated discharging current (TSDC) curves for the various samples were measured. The results showed a certain scatter and Fig. 13A shows the curve for sample (7) as a representative result. At first glance one cannot attribute the TSDC to pyroelectric activity since the total charge released by thermal stimulation is quite high, about 800 $\mu C/cm^2$, as compared to ~40 $\mu C/cm^2$, typically for PZT. However, the frozen-in defect-dipoles can be released by thermal activation and consequently prevail itself as anomalous TSDC.

After quenching (structural depinning), the defect-dipoles are randomly distributed. However, they can be oriented by the externally applied electric field at high temperature. After ageing the defect-dipoles are already oriented by the ferroelectric polarization and they have no depolarization effect. As a consequence, the TSDC curve, Fig. 13B, has a totally different profile. It shows only one single peak at the typical Curie transition temperature (~315 °C). The total charge released in both cases is almost constant (~800 $\mu C/cm^2$) confirming that the direction of the ferroelectric polarization and defect-dipoles in poled samples after de-ageing is the same. Similar behaviour was observed previously.[17,37,38,2]

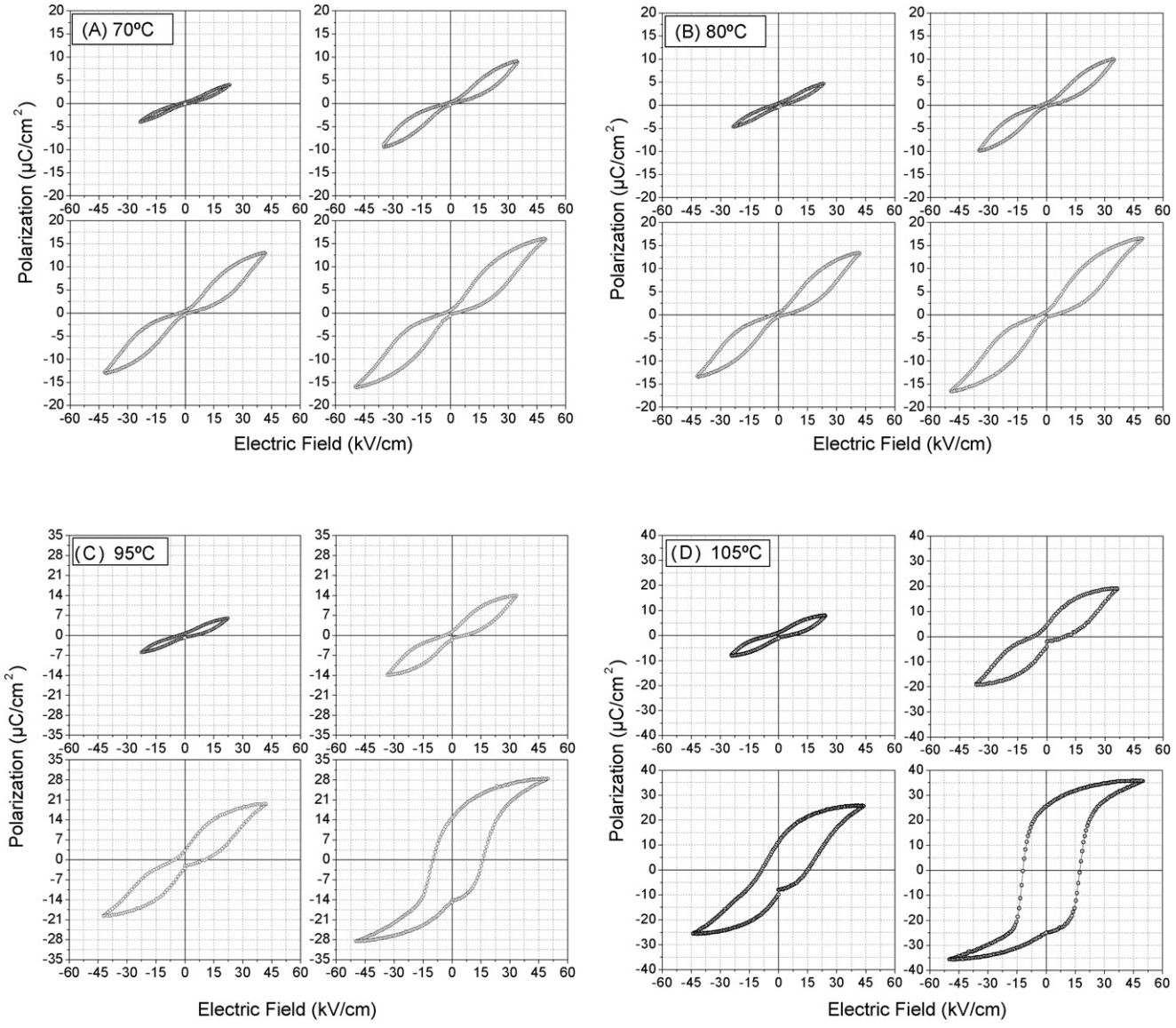

Fig. 6. Hysteresis loops for increasing maximum electric fields of a non-poled samples at (A) 70 °C, (B) 80 °C, (C) 95 °C, (D) 105 °C.

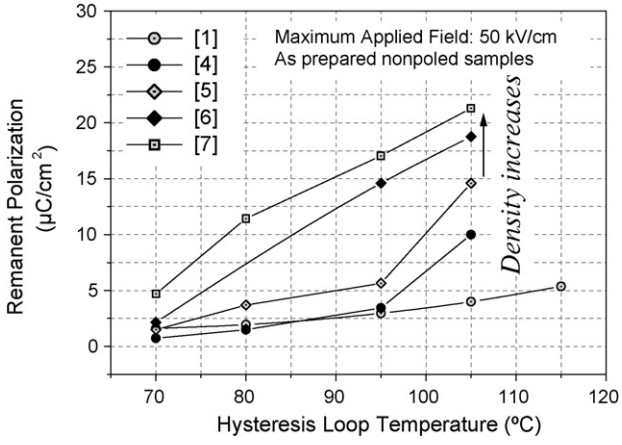

Fig. 7. Hysteresis loops opening as a function of temperature for different densities.

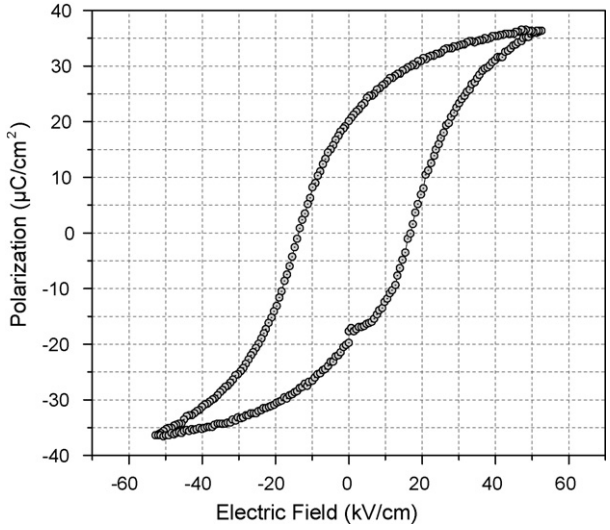

Fig. 8. Hysteresis loop at room temperature after quenching.

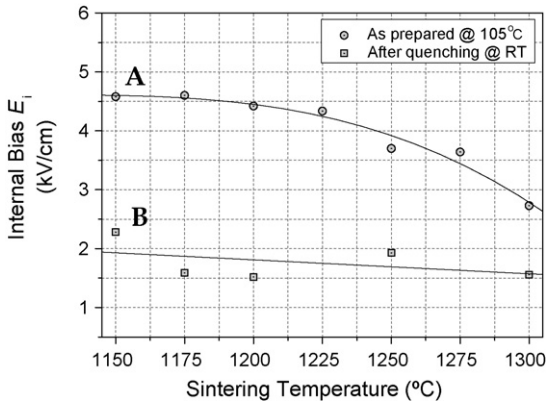

Fig. 9. Internal bias E_i after electrical (A) and thermal (B) de-ageing.

4. Discussion

4.1. Ageing phenomena

Ageing phenomena are observed in all ferroelectrics. It usually manifests itself by a double *P–E* hysteresis loop in nonpoled samples, a decrease of the dielectric constant at a small ac electric field and piezoelectric constant at small mechanical stress. The theory of ferroelectricity cannot directly explain ageing behaviour.

It is natural to speculate that ferroelectric ageing is caused by a certain relaxation process. Generally, it is agreed that ageing can be phenomenologically attributed to a gradual *stabilization* of the domain pattern by $D'_{Zr/Ti}$ $-V_O^{\bullet\bullet}$ defect-dipoles. This argument is widely verified, theoretically[1,16,20–23] and experimentally.[41–44] However, Dimos and co-workers[25–28] have shown that, pinning can also be of electronic origin due to locking of domains by electronic charge trapping centres. The central controversy is, still, whether the domain stabilization stems from a domain effect or a volume effect and whether it is ionic or electronic. For the domain effect, it is believed that defects migrate to the domain walls during ageing and consequently pin the domain walls. For the volume effect, it is considered that the defect-dipoles align along the spontaneous-polarization P_S orientation over the whole domain during ageing and thus make domain switching difficult. In the domain effect, however, the existence of domain walls is a necessary condition for ageing. However, in the volume effect model, ageing is expected to exist even in a single-domain sample. On this assumption, Zhang and Ren[45] prepared a single-domain BT single crystal and showed that ageing still occurs. Therefore, they concluded that the volume effect rather than domain-wall pinning is the governing mechanism for ferroelectric hysteresis loop pinning. As it is impossible to distinguish between different mechanisms which cause the stabilization from purely electrical measurements,[27,28] we will also assume that the volume effect can explain our results.

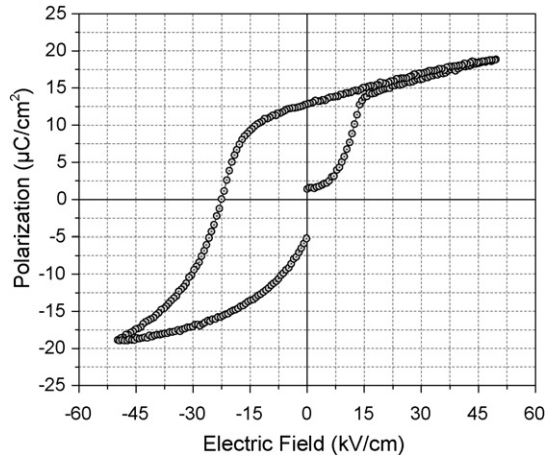

Fig. 10. Hysteresis loop at room temperature for a sample poled at 30 kV/cm and 90 °C after electrical de-ageing (50 kV/cm, 105 °C).

The model of ageing phenomena, as initially set by Carl and Härdtl[22] and adopted by many others[43–46] is based on the fact that the PZT perovskite structure contains $V_O^{\bullet\bullet}$ vacancies and $Fe'_{Zr/Ti}$ $-V_O^{\bullet\bullet}$ defect-dipoles. Now we consider the symmetry of the statistical distribution[43] of $V_O^{\bullet\bullet}$ around a $Fe'_{Zr/Ti}$. In the cubic paraelectric phase, Fig. 14A, the defect probabilities P_v of finding an $V_O^{\bullet\bullet}$ on the neighbouring, equivalent sites (1, 2, 3, 4) of the $Fe'_{Zr/Ti}$ are the same ($P_{v1} = P_{v2} = P_{v3} = P_{v4}$). Thus, the symmetry of the equilibrium defect probability around $Fe'_{Zr/Ti}$ is cubic, following the cubic crystal symmetry of the paraelectric phase. In the ferroelectric phase, Fig. 14C, the polar tetragonal symmetry renders the sites 1 and 2 equivalent but inequivalent to sites 3 and 4 and thus the defect probabilities P_v are $P_{v1} = P_{v2} \neq P_{v3} \neq P_{v4}$.

Consider a macroscopic crystal in the cubic, paraelectric phase in equilibrium, Fig. 14A. Upon cooling, the crystal undergoes a paraelectric–ferroelectric (PE–FE) phase transition transforming into a multidomain tetragonal ferroelectric phase, Fig. 14B. The resulting spontaneous polarization P_S lowers abruptly the symmetry but the defects cannot move quickly since the PE–FE phase transition is diffusionless. As a result, the polar tetragonal ferroelectric phase inherits a cubic defect-symmetry after the transition, Fig. 14B. However, this *fresh* ferroelectric phase, Fig. 14B, is not a stable state because the defect symmetry (cubic) does not match the crystal symmetry (tetragonal).[16] Given sufficient time (and energy), defect/vacancy re-distribution occurs[16] and the cubic defect symmetry will be changed into a polar tetragonal one, Fig. 14C. Such a process involves a short-range migration of ions/vacancies. Sites 3 and 4 are no longer equivalent because site 3 is closer to the ion on site 0. Thus, the site closer to the $Fe'_{Zr/Ti}$ has a higher defect probability due to the Coulomb attractive force between the effectively negatively $Fe'_{Zr/Ti}$ and effectively positively $V_O^{\bullet\bullet}$. This process requires some time to complete. This is the microscopic mechanism of *ageing* (domain wall pinning) in ferroelectrics.

After ageing, the defect symmetry in each domain follows the polar tetragonal crystal symmetry. The configuration of $Fe'_{Zr/Ti}$ and $V_O^{\bullet\bullet}$ exhibits a defect-dipole moment P_D following the spontaneous polarization P_S direction[40] of the residing domain, Fig. 14C1. Now every domain is in its stable state. When such stable domains are switched by an electric field, domain

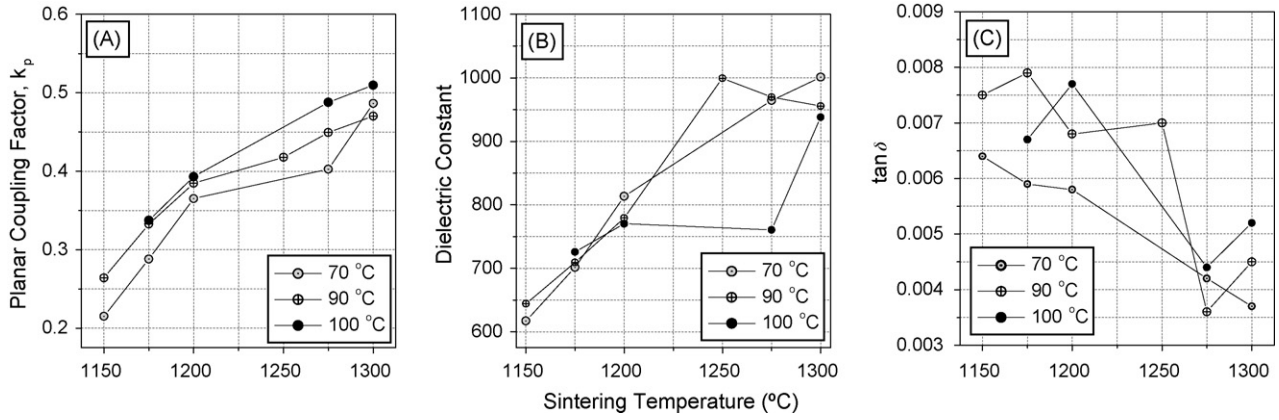

Fig. 11. (A–C) Dielectric and piezoelectric parameters after normal poling (before de-ageing).

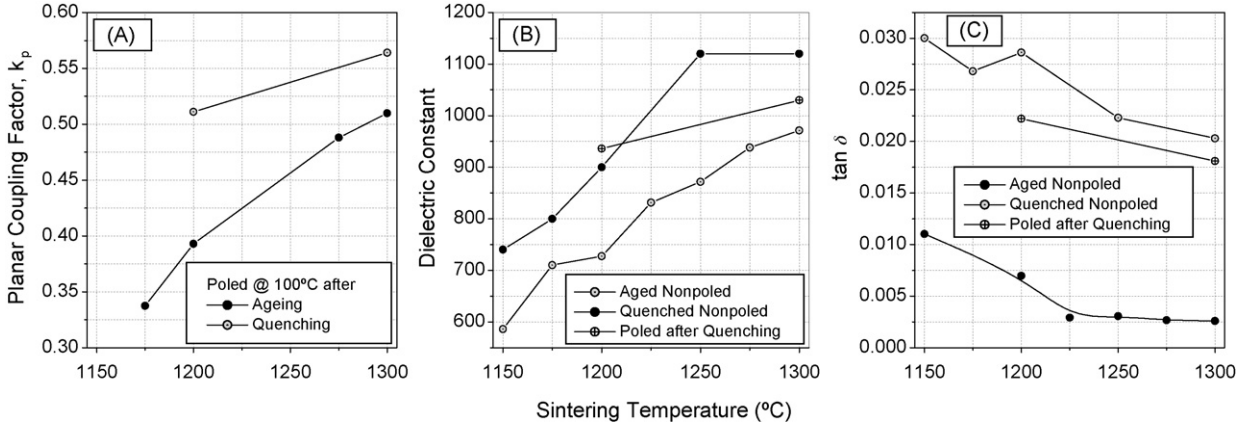

Fig. 12. (A–C) Dielectric and piezoelectric parameters before and after thermal de-ageing.

switching occurs abruptly (*without diffusion*) with the spontaneous polarization following the field direction, Fig. 14C2. However, the defect-dipole cannot be rotated in such a diffusionless process, or, in other words, not switched. Therefore, the defect-dipole provides a restoring force or a reverse internal field favouring to switch back the domain when the electric field is removed, Fig. 14C1 and C2. As a consequence, the original domain pattern is restored so that the defect symmetry and dipole moment follow those of the crystal symmetry in every domain. Consequently a pinched hysteresis loop in the *P–E* relation is observed as well as a shift in the *E*-axis due to the existence of P_D.[44]

4.2. Thermal de-ageing

As discussed, upon quenching and immediately after the PE–FE phase transition the oxygen vacancies adopt the cubic symmetry. This de-aged configuration is analogous to the fresh state, Fig. 14B. At this stage we have two directions to go. Either to let the material age and follow the same scenario we mentioned before or we apply strong poling conditions. In the latter way the domains will be oriented easily without the hindrance of the defects since the defect polarization is still zero, Fig. 14D. So far, even after removing the field, the defects have no influence and remain in the cubic symmetry. Consequently, there

Table 2
Dielectric and piezoelectric parameters at different poling conditions

Samples	Aged nonpoled		Directly poled			Poled after electrical de-ageing			Nonpoled after quenching		Poled after quenching		
	ε_r	Tan δ	ε_r	Tan δ	k_p	ε_r	Tan δ	k_p	ε_r	Tan δ	ε_r	Tan δ	k_p
(1)	585	0.01103	582	0.0071	0.274				740	0.030			
(2)	710					730	0.0067	0.337	800	0.0268			
(3)	730	0.00696	745	0.0084	0.382	770	0.0077	0.393	900	0.0286	936	0.0222	0.511
(4)	830	0.00292											
(5)	875	0.00305							1120	0.0223			
(6)	940	0.00267				760	0.0044	0.49					
(7)	975	0.00259	955	0.0052	0.496	940	0.0052	0.51	1120	0.0203	1030	0.0181	0.564

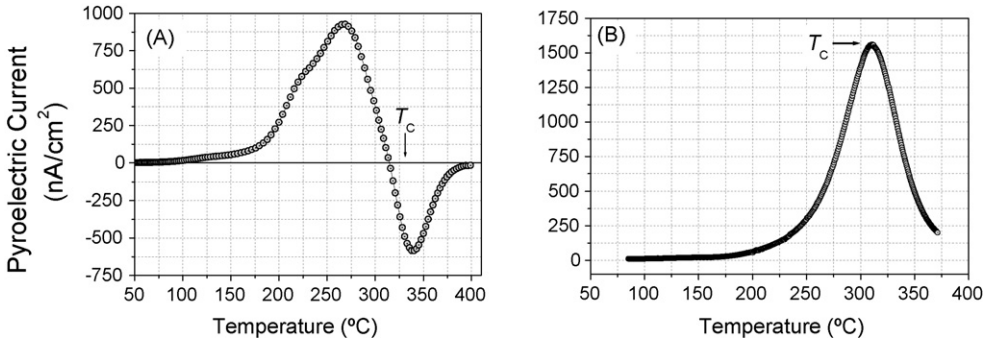

Fig. 13. Thermal stimulated discharge current (TSDC) for samples poled after (A) electrical de-ageing and (B) thermal de-ageing.

is no restoring force to switch the oriented domains back. In time the oxygen vacancies will migrate by diffusion following the host crystal symmetry and the spontaneous polarization P_S. However, such diffusion redistribution of defects will not affect the domain orientation because defect-dipoles are following the ferroelectric polarization direction. This new domain stability can be sketched as in Fig. 14E. Fig. 10 also shows a good verification of this assumption. The anomalous hysteresis loops show a unipolar polarization orientation for poled samples after de-ageing. De-ageing directly followed by poling results in irreversible changes in the defect distributions and domain stability.[35,36] This simple explanation also enables us to understand the large enhancement in the piezoelectric coupling factor k_p after the same conditions of poling right after quenching, since the defects have no chance to age and thereafter to dominate.

4.3. Pyroelectric behaviour

4.3.1. Before de-ageing

In the aged state, the sample is still not fully polarized as can be recognized from the value of the k_p, implying that the majority of the domains are still pinned. The oriented domains are in fact in an unstable state because the defect polarization P_D does not follow the spontaneous polarization P_S of the oriented domains. That means that the defect-dipole moment P_D can memorize the original crystal domain patterns after ageing, and does not change during subsequent domain switching.[44] However, under thermal activation defects can migrate by diffusion in order to match the crystal symmetry. This motion of defects, primarily the oxygen vacancies $V_O^{\bullet\bullet}$, produces a current, which is opposite to the intrinsic thermal depolarization current, which has also just started to contribute. At this point we have two types of current of different nature and direction. The intrinsic pyrocurrent which is rising in the positive direction and the extrinsic diffusion current of the oxygen vacancies which rising in the negative direction and counteracting the pyrocurrent to peak at a lower temperature (250 °C) than the typical Curie temperature (∼330 °C), Fig. 13A. By approaching the Curie transition temperature, the pyrocurrent vanishes whereas the diffusion motion of the defects may continue in the negative direction. The reason for that is the material undergoes a FE–PE phase transition, which is fast in nature while the defects move by (slow) diffusion. Thus, it takes a relatively long time to adapt to the new (cubic) crystal symmetry. Consequently its current vanishes at relatively higher temperature (400 °C).

4.3.2. After thermal de-ageing

The thermally stimulated discharge current (TSDC) curve, as shown in Fig. 13B, of a poled sample after quenching can be explained as follows. After quenching, as we illustrated previously, strong poling for a sample in the fresh quenched state can easily and permanently orient the domains. Although the oxygen vacancies still have a cubic symmetry, they have no influence on the oriented domain walls even after ageing by diffusion.

By short circuiting the sample with an electrometer and applying a constant heating rate, we expect two types of discharge current: the defect-dipole discharge current and the intrinsic depolarization current. This was indeed experimentally observed and we found an extremely high and broad TSDC curve peaking at the typical Curie transition temperature (∼330 °C). At this point we have two important observations. Firstly, the single peak in the TSDC profile enhances the idea that the defect-dipoles are not misaligned with the intrinsic ferroelectric polarization and ageing is not going towards depolarization. This is also consistent with a normal hysteresis loop observed at room temperature after quenching. Secondly, the extremely high TSDC can be understood now as a combination of two discharging currents and accordingly the real spontaneous polarization P_S cannot be determined by this measurement.

4.4. Dielectric loss

In ferroelectric materials, all properties are closely linked. The ferroelectric *P–E* hysteresis behaviour can give valuable information on the different physical processes that take place in ferroelectric materials, e.g. domain-wall pinning, defect ordering, and nature of defects.[1,18] Having a mechanism explaining the pinched hysteresis loops, helps to interpret the other dielectric, piezoelectric and pyroelectric properties.

4.4.1. Aged samples

Herbiet et al.[47] stated that the extrinsic (domain wall) contribution is the main source of the dielectric loss because the domain wall motion can induce mechanical friction. The extrinsic contribution can be as much as 70% of the total loss at room temperature.[47]

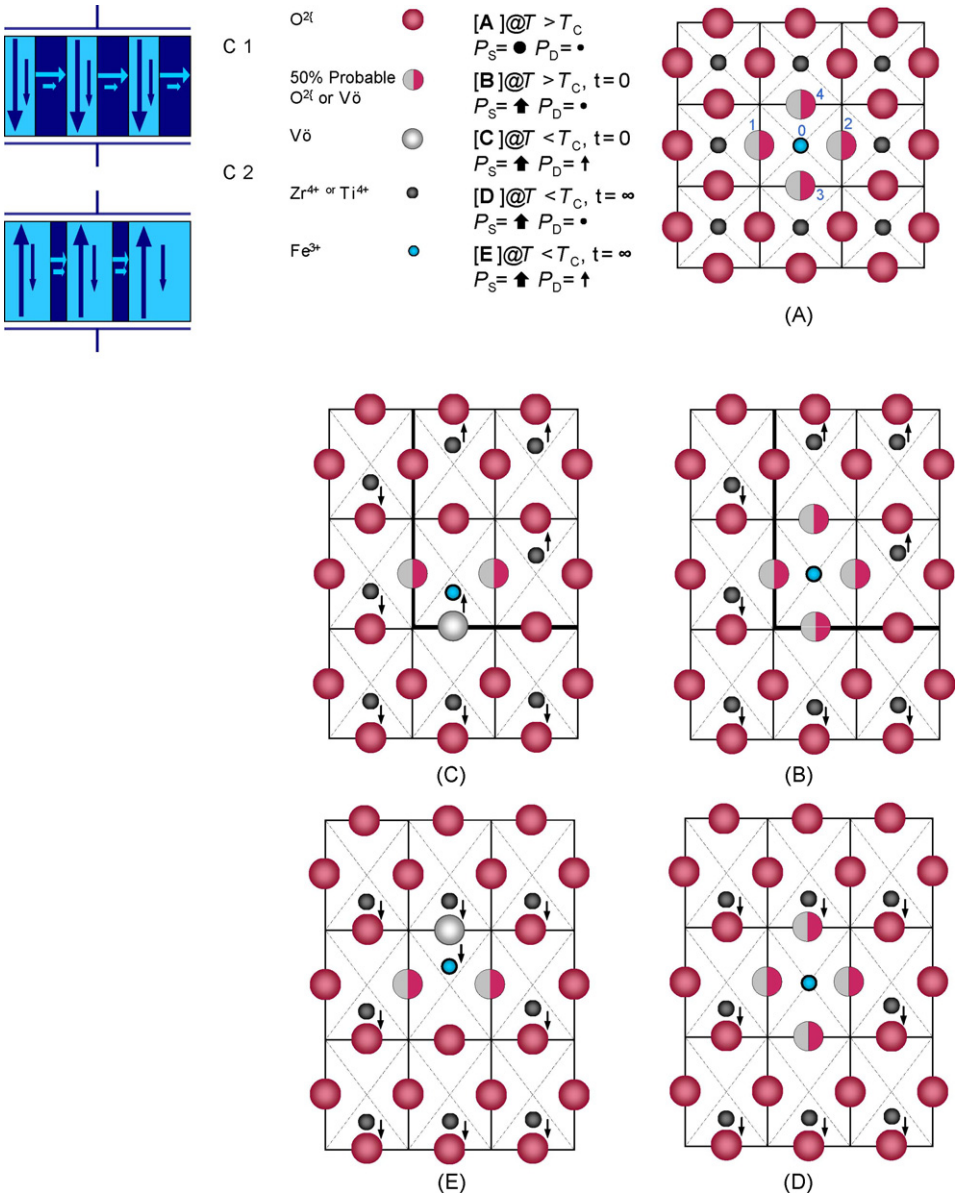

Fig. 14. Symmetry-conforming property of point defects. A typical ABO_3 (PZT) perovskite structure is considered, which contains an O^{2-} vacancy and an acceptor impurity Fe^{3+} occupying the (Zr^{4+}, Ti^{4+}) site. The probability P_{vi} refers to the conditional probability of finding an O^{2-} vacancy and O^{2-} ion at the site i ($i = 1, 2, 3, 4$), respectively, when an impurity ion Fe^{3+} occupies site 0. (A) A configuration represents a non-polar/centrosymmetric cubic paraelectric state ($T > T_C$). (B) Fresh (unaged) polar tetragonal ferroelectric state ($T < T_C$) (thick line represents the domain wall). (C) Polar tetragonal ferroelectric state after O^{2-} vacancy diffusion. (C1) A stable multidomain structure of the tetragonal ferroelectric crystal after ageing in the ferroelectric state, in which defect symmetry follows crystal symmetry in every domain. (C2) Unstable state after domain switching by electric field E. Double hysteresis loop (P–E curve) during reversible domain switching between (C1) and (C2). Stable states are those where the defect symmetry matches the crystal symmetry; unstable states are those where they do not match. (D) Poled configuration in the fresh state before ageing dominates, in which the defect symmetry matches the crystal symmetry. Even upon the inevitable diffusion motion of the oxygen vacancies (E), the poled configuration (*i.e.* the stable state) is still preserved.

Before poling the domain walls are pinned by defects leading to restricted movement of the domain walls (assuming the movement of the domain walls is the main contribution to the dielectric loss). Consequently, a low dielectric loss is expected.[21,48] Poling of a hard ferroelectric does not greatly reduce the domain wall number (see Fig. 14C1 and C2), as evidenced by the pinched hysteresis loop. However, there is a significant movement of domain walls due to poling. As a result of pinning, which acts as an elastic restoring force, the domain walls in time return back. Accordingly, the dielectric loss increases after poling contrary to the common behaviour. The same thought is also applicable for poled ceramics after electrical de-ageing. Because the material in this case is more polarized than before electrical de-ageing, the increase in tan δ is less, see Table 3.

4.4.2. *Thermally de-aged samples*

After quenching and before ageing (*i.e.* before defect-dipoles develop) the material can be relatively easy poled leading to a reduction in the number of domain walls, which are now pinned by the global ferroelectric polarization. Consequently, after pol-

Table 3
Schematic of the dielectric loss (tan δ) behaviour

	Before poling	After poling
Aged	↓	↑
Electrically de-aged	↓	↑
Thermally de-aged	↑	↓

ing the material shows domain wall stability and lower dielectric loss. Moreover, a remarkable increase in the electromechanical coupling factor k_p is observed. The explanation given is again based on the assumption that the major contribution to the loss is the domain wall motion.

5. Conclusions

Poling of hard ferroelectric ceramics cannot be accomplished before domain wall depinning. The restriction on domain wall mobility can be released by applying a high temperature and high periodic electric field before a normal poling procedure. Another, more efficient, way for domain wall depinning is quenching from a relatively high temperature where after the material showed remarkably improved piezoelectric properties. The pyroelectric current can be used as monitoring tool to indicate to the degree of domain pinning by defects. The dielectric loss behaviour is consistent with the degree of pinning.

References

1. Damjanovic, D., *The Science of Hysteresis*, *Vol. 3*, ed. I. Mayergoyz and G. Bertotti. Elsevier, 2005.
2. Okazaki, K., *Jpn. J. Appl. Phys.*, 1993, **32**, 4241.
3. Zhong, W. L., Wang, Y. G., Yue, S. B. and Zhang, P. L., *Solid State Commun.*, 1994, **90**, 383.
4. Kamel, T. M., Kools, F. X. N. M. and de With, G., *J. Eur. Ceram. Soc.*, 2006, **27**, 2471.
5. Ueda, I. and Ikegami, S., *Jpn. J. Appl. Phys.*, 1968, **7**, 236.
6. Cai, S., Xu, Y., Millar, C. E., Pedersen, L. and Sorensen, O., *IEEE*, 1995, 804.
7. Bryant, P. and Palmer, T., *J. Aust. Ceram. Soc.*, 2000, **36**, 153.
8. Nagata, H. and Takenaka, T., *IEEE*, 2001, 45.
9. Lente, M. H. and Eiras, J. A., *J. Appl. Phys.*, 2001, **89**, 5093.
10. Yamada, A., Chung, Y., Takahashi, M. and Ogawa, T., *Jpn. J. Appl. Phys.*, 1996, **35**, 5232.
11. Ogawa, T. and Nakamura, K., *Jpn. J. Appl. Phys.*, 1998, **37**, 5241.
12. Ogawa, T., *Ferroelectrics*, 2000, **240**, 75.
13. Ogawa, T., *Jpn. J. Appl. Phys.*, 2000, **39**, 5538.
14. Ogawa, T., *Jpn. J. Appl. Phys.*, 2001, **40**, 5630.
15. Ogawa, T., *Ferroelectrics*, 2002, **273**, 371.
16. Arlt, G. and Neumann, H., *Ferroelectrics*, 1988, **87**, 109.
17. Jaffe, B., Cook, W. R. and Jaffe, H., *Piezoelectric Ceramics*. Academic Press, New York, 1971.
18. Lines, M. E. and Glass, A. M., *Principles and Applications of Ferroelectrics and Related Materials*. Oxford, Clarendon, 1979.
19. Morosov, M., Softening and Hardening Transitions in Ferroelectric $Pb(Zr,Ti)O_3$ Ceramics. PhD Thesis. EPFL, Lausanne, Switzerland, 2005.
20. Lambeck, P. V. and Jonker, G. H., *J. Phys. Chem.*, 1986, **47**, 453.
21. Schulze, W. A. and Ogino, K., *Ferroelectrics*, 1988, **87**, 361.
22. Carl, K. and Härdtl, K., *Ferroelectrics*, 1978, **17**, 473.
23. Robels, U. and Arlt, G., *J. Appl. Phys.*, 1993, **73**, 3454.
24. Robels, U., Calderwood, J. H. and Arlt, G., *J. Appl. Phys.*, 1995, **77**, 4002.
25. Dimos, D., Warren, W. L., Sinclair, M. B., Tuttle, B. A. and Schwartz, R. W., *J. Appl. Phys.*, 1994, **76**, 4305.
26. Warren, W. L., Dimos, D., Tuttle, B. A., Nasby, R. D. and Pike, G. E., *Appl. Phys. Lett.*, 1994, **65**, 1018.
27. Dimos, D., Warren, W. L. and Al-Shareef, H. N., In *Thin Film Ferroelectric Materials and Devices*, ed. R. Ramesh. Kluwer Academic Publishers, 1997, p. 199.
28. Warren, W. L., Tuttle, B. A. and Dimos, D., *Appl. Phys. Lett.*, 1995, **67**, 1426.
29. Uchino, K., *Ferroelectric Devices*. Marcel Dekker, 2000.
30. Tagantsev, A. K., Stolichnov, I., Colla, E. L. and Setter, N., *J. Appl. Phys.*, 2001, **90**, 1387.
31. Lang, S. B., *Source Book of Pyroelectricity*. Gordon and Breach Science Publishers, London, 1974.
32. Li, B., Zhu, Z., Li, G., Yin, Q. and Ding, A., *Jpn. J. Appl. Phys.*, 2004, **43**, 1458.
33. Wu, L., Wei, C.-C., Wu, T.-S. and Liu, H.-C., *J. Phys.*, 1983, **16**, 2813.
34. Li, B., Li, G., Yin, Q., Zhu, Z., Ding, A. and Cao, W., *J. Phys.*, 2005, **38**, 1107.
35. Tan, Q., Xu, Z. and Viehland, D., *J. Mater. Res.*, 1999, **14**, 465.
36. Kohli, M., Muralt, P. and Setter, N., *Appl. Phys. Lett.*, 1998, **72**, 3217.
37. Blood, H. L., Levine, S. and Roberts, N. H., *J. Appl. Phys.*, 1956, **27**, 660.
38. Northrip, J. W., *J. Appl. Phys.*, 1960, **31**, 2293.
39. Pandey, S. K., Thakur, O. P., Kumar, A. and Prakash, C., *J. Appl. Phys.*, 2006, **100**, 014104.
40. Lohkämper, R., Neumann, H. and Arlt, G., *J. Appl. Phys.*, 1990, **68**, 4220.
41. Yang, T. J., Gopalan, V., Swart, P. J. and Mohideen, U., *Phys. Rev. Lett.*, 1999, **82**, 4106.
42. Chou, C.-C., Hou, C.-S. and Yeh, T.-H., *J. Eur. Ceram. Soc.*, 2005, **25**, 2505.
43. Ren, X., *Nat. Mater.*, 2004, **3**, 91.
44. Zhang, L. and Ren, X., *Phys. Rev.*, 2005, **B71**, 174108.
45. Zhang, L. and Ren, X., *Phys. Rev.*, 2006, **B73**, 094121.
46. Liu, W., Chen, W., Yang, L., Zhang, L., Wang, Y., Zhou, C., Li, S. and Ren, X., *Appl. Phys. Lett.*, 2006, **89**, 172908.
47. Herbiet, R., Robels, U., Dederichs, H. and Arlt, G., *Ferroelectrics*, 1989, **98**, 107.
48. Yoon, S.-J., Joshi, A. and Uchino, K., *J. Am. Ceram. Soc.*, 1997, **80**, 1035.